# Supporting Information

## Diacetylene mixed Langmuir monolayers for interfacial polymerization

Luisa Ariza-Carmona,  Carlos Rubia-Payá, María T. Martín-Romero,
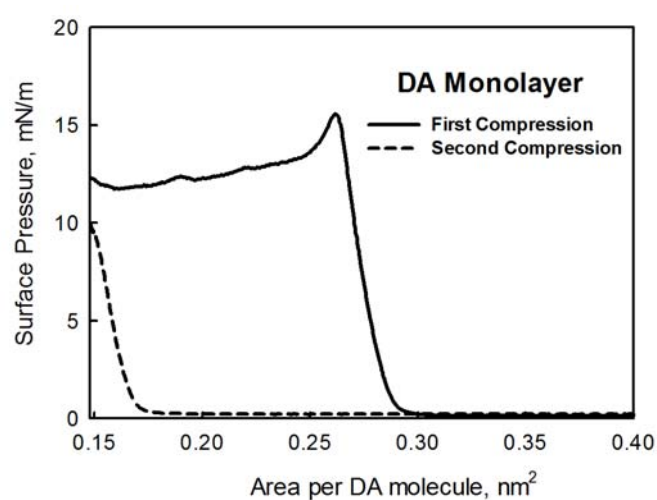
Juan J. Giner-Casares, and Luis Camacho

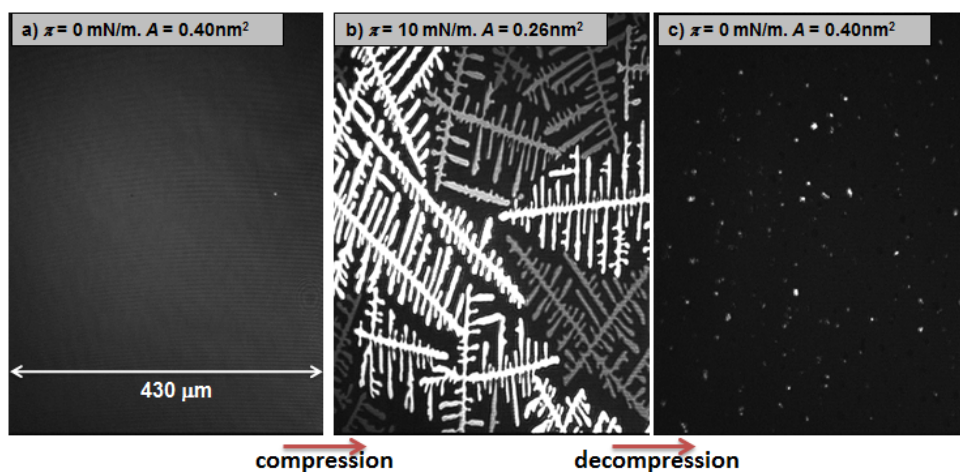**Figure S1**: Cyclic π-A isotherms of DA monolayer.



**Figure S2**: BAM images of the pure DA Langmuir monolayers during the compression and decompression process.
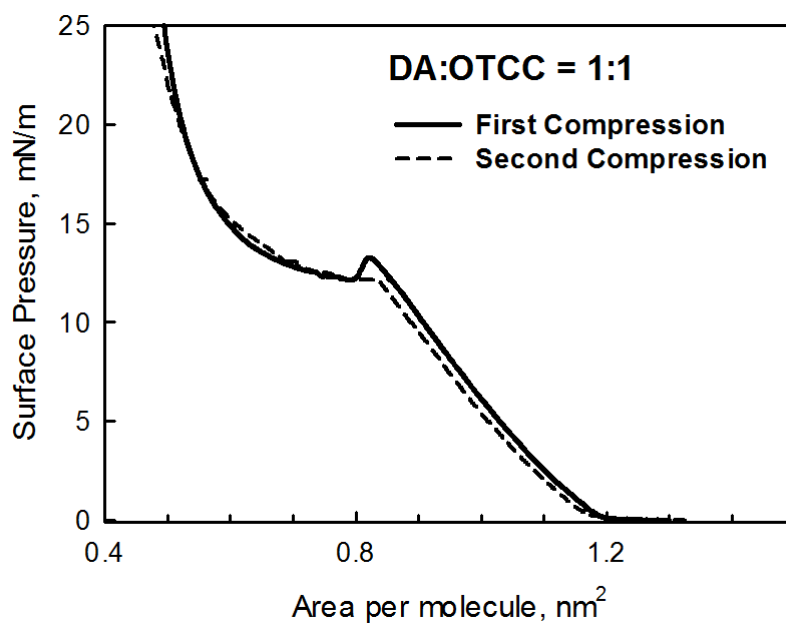
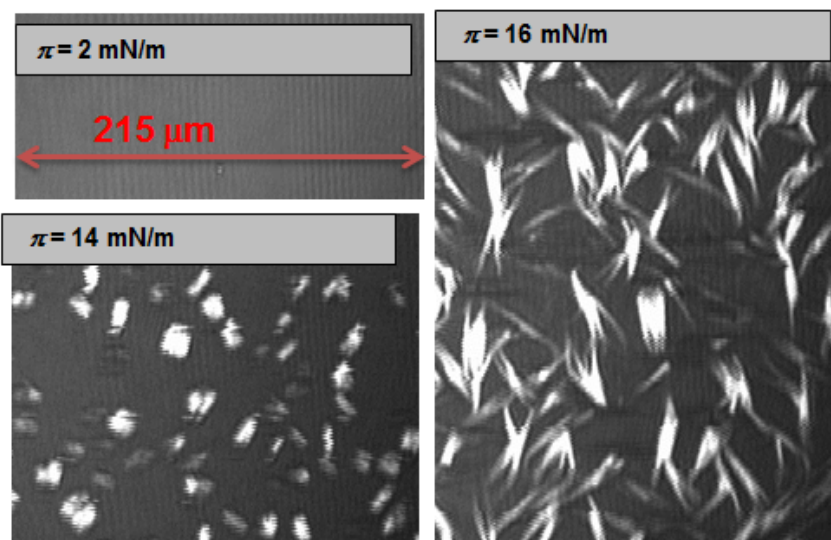**Figure S3**: Cyclic $\pi$-A isotherms of DA:OTCC = 1:1 monolayer.



**Figure S4**: BAM images of the pure OTCC Langmuir monolayers acquired at different values of surface pressure, as indicated in the Figure.
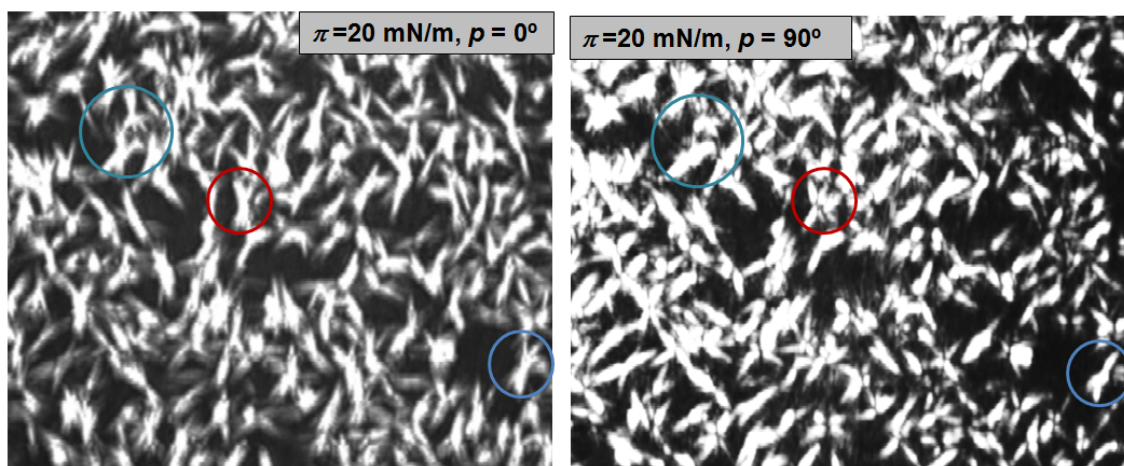
**Figure S5.** BAM images of the mixed DA:OTCC mixed Langmuir monolayer prior to the polymerization. The BAM pictures have been recorded on the same region of the air/water interface while changing the polarizer from 0° to 90°. The circles highlight common points that allow identifying the different regions.



**Figure S6.** BAM images of the DA:OTCC mixed Langmuir monolayer after the polymerization. The BAM pictures have been recorded at the same region of the air/water interface while changing the polarizer from 60° to 30°. The circles highlight common points that allow identifying the different regions.
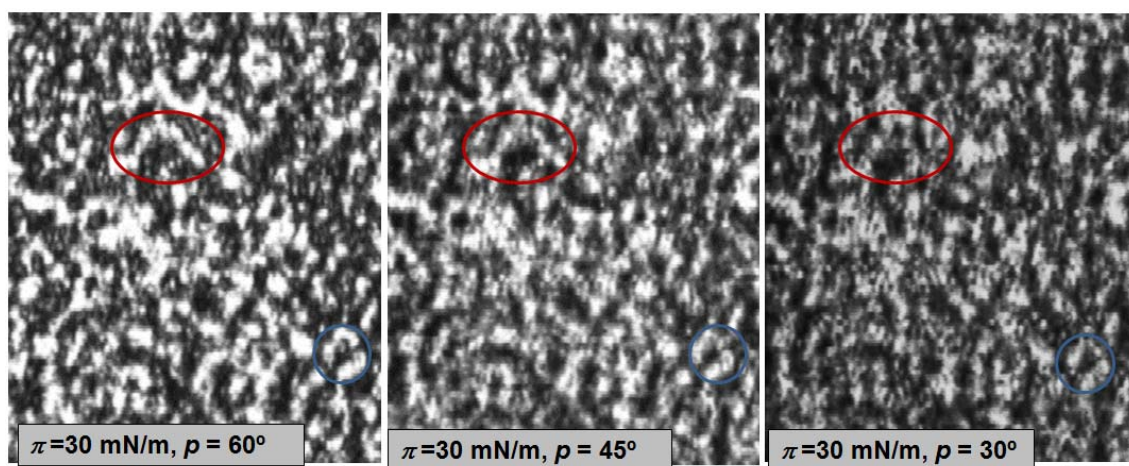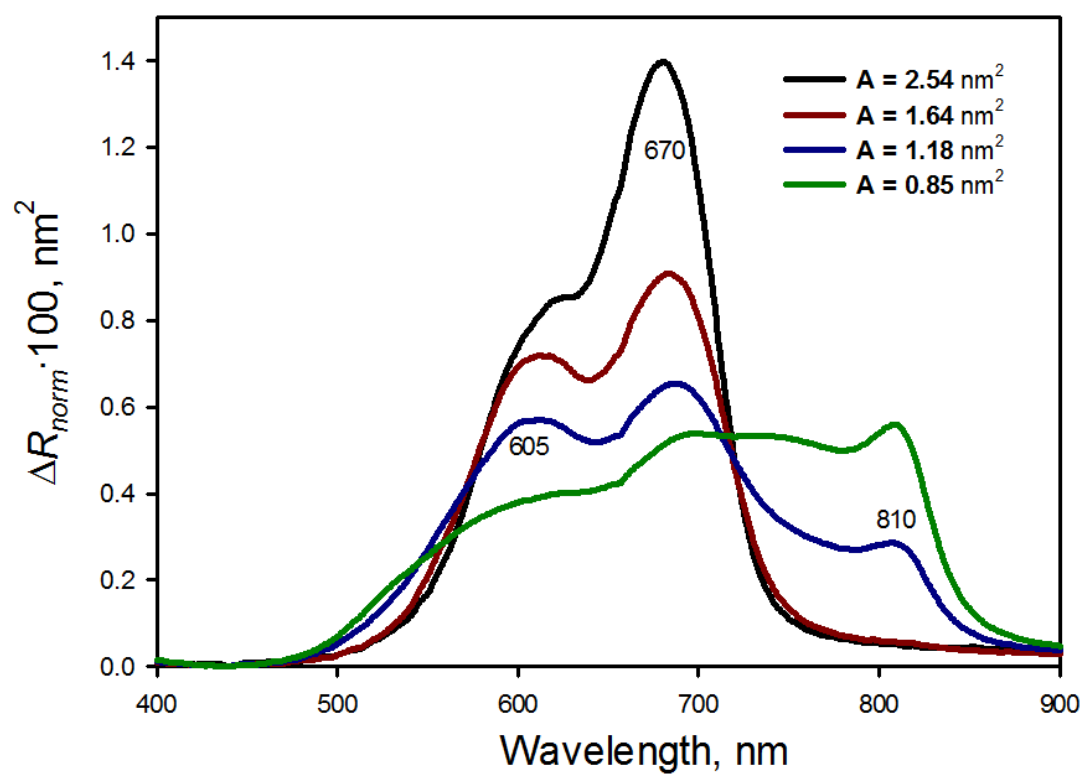
**Figure S7:** Normalized UV-vis reflection spectra of the pure OTCC Langmuir monolayer at different surface areas, as indicated within the Figure.

**Molecular Mechanics Study of the PDA:OTCC system.**

A single polymer chain segment consisting of six DA⁻ monomers was built ($C_{152}H_{254}O_{12}$, see Figure S5) for studying the PDA:OTCC mixed monolayer. The polymer segment was built in the aligned conformation, $\theta_\alpha = \theta_\beta = 180°$, where $\theta_\alpha$ is the torsion angle formed by the following atoms; C‒C‒C$_\alpha$‒C$_\alpha$' $\theta_\beta$ is defined with respect to atoms C‒C‒C$_\beta$‒C$_\beta$' (see Figure S8). The six carboxylic groups are dissociated (total charge of -6). Length and bond angles were introduced using the HyperChem Model Build database. Alkyl chains, R1 and R2 (see Figure S8), were arranged in all-trans configuration. The charge distribution was assigned using the AM1 semiempirical method. A similar procedure was performed for the modeling of the OTCC⁺ molecule.
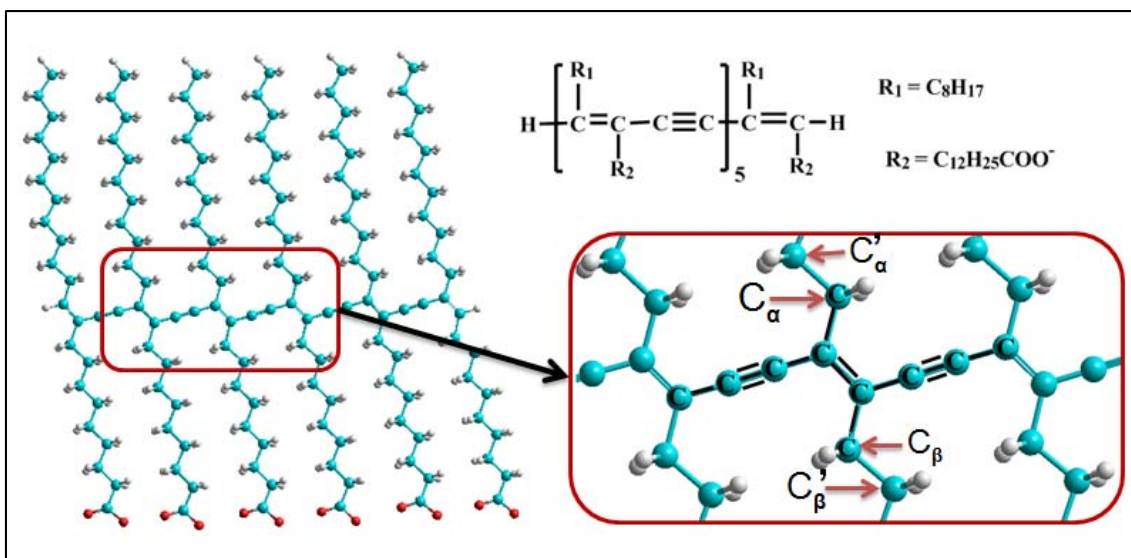


**Figure S8**: Composition of the polymer segment for the study of the mixed PDA:OTCC mixed Langmuir monolayer.

A set of six OTCC molecules were positioned parallel with an intermolecular distance of ca. 0.4 nm approximately using a H-configuration. The PDA polymer segment was placed between the OTCC alkyl chains. Figure S9a shows two views (top and side) of the complex initial structure before geometry optimization.

After building the mentioned model, the PDA:OTCC complex geometry was optimized by MM+. Other structures with lower energy were checked by performing three runs of molecular dynamics simulations. Each run consisted of heating the structure to 400 K, running a molecular dynamics simulation for 5 ps, and then annealing to 0 K. Finally, the resulting structure was again optimized by using MM+ (RMS gradient 0.001kcal/Å×mol). Figure S9b shows two views (top and side) of the complex final structure after geometrical optimization. The geometry optimization procedure was repeated 4 times, starting from slightly different starting positions. No significant differences in the final structures was observed.
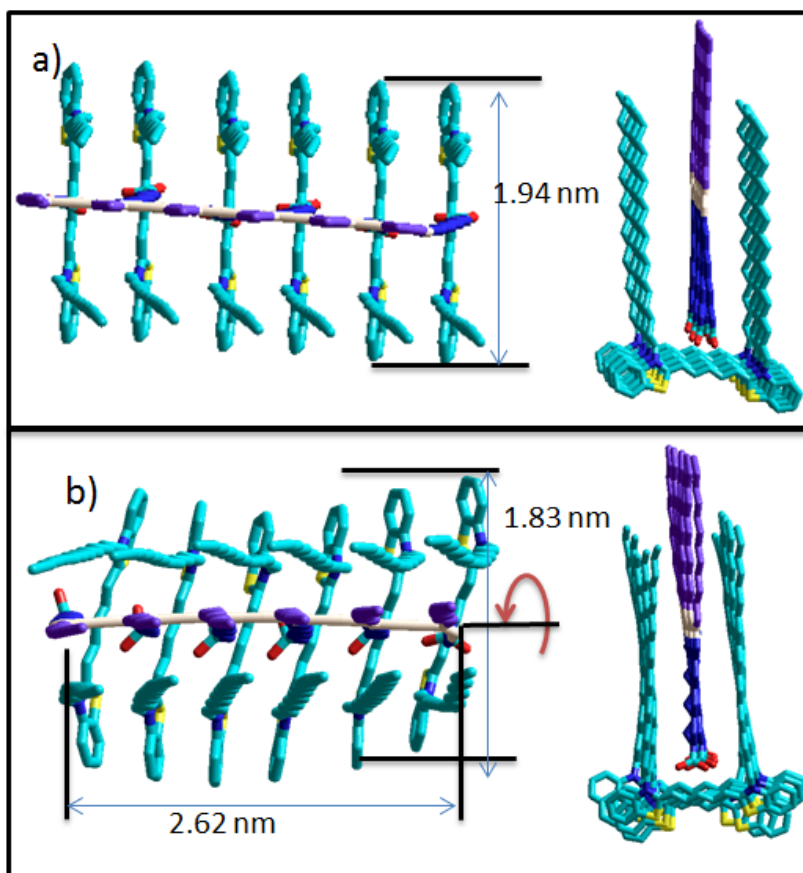
**Figure S9**: a) Top and side perspectives of the PDA:OTCC initial structure before the geometry optimization. b) Top and side perspectives of the complex final structure after the geometry optimization. The PDA alkyl chains are represented by violet and blue color, and the conjugation plane is represented by gray color.

The optimized complex structure displays angle values of $\theta_\alpha = 175°\pm2°$, and $\theta_\beta = 178°\pm2°$. Additionally, a certain degree of rotation is observed in the polymer conjugation plane (see Figure S9). Such rotation can be analyzed, taking into account the torsion angle formed between consecutive double $C = C$ (see section 8, Supporting Information). Thus, we obtain that the dihedral angle between consecutive double bonds, $C=C\bullet\bullet\bullet C=C$, is $176° \pm 2°$. In addition, such rotation is always in the same direction leading to a helical structure (worm-like chain). In the complex final structure, the total rotation of the conjugation plane is ca. 24°. However, the PDA alkyl chains are partially tiltled for compensating such rotation, retaining an aligned final structure between the alkyl chains and the polymer chain.

The OTCC polar group is partially twisted to minimize their interaction energy with the carboxylic group, reducing its length from 1.94 to 1.83 nm (see Figure S9). The total area occupied by the polar group for this structure is ca. 4.8 nm². The average spacing between DA or OTCC units is 2.62 / 5 = 0.52 nm. Taking into account that there are 18 alkyl chains per complex unit, an area of ca. 0.27 nm² per alkyl chain is obtained. This area is close to the experimental value obtained from the isotherm, ca. 0.25 nm² per alkyl chain).

As a reference, the structure of the DA:OTCC system without polymerization is studied. First, the DA:OTCC pair was optimized as described in manuscript (see Scheme 1G for the optimized structure). Next, six DA:OTCC pairs were positioned parallel with an intermolecular distance of ca. 0.5 nm using a H-configuration. After building the mentioned model, the DA:OTCC complex geometry was again optimized. The optimized complex structure is show in Figure S10. The average spacing between DA or OTCC units is ca. 0.54 nm.

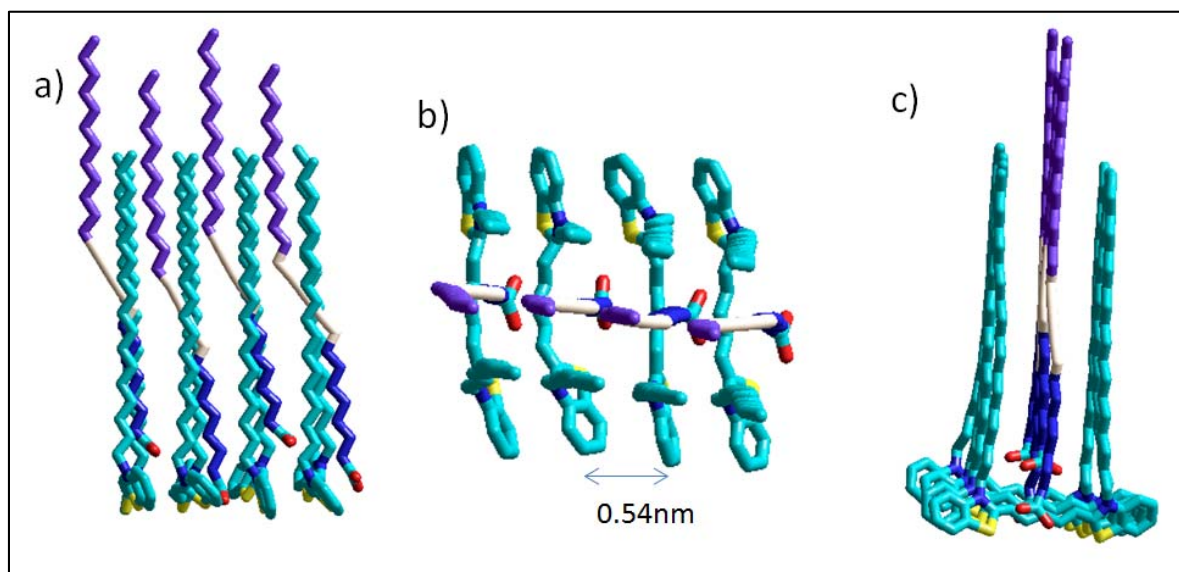

**Figure S10**: a) side, b) top and c) frontal perspectives of the DA:OTCC complex structure after the geometry optimization. The DA alkyl chains are represented by violet and blue color. Diacetyle group is represented by gray color.

**PDA Molecular Mechanics Study.**

The polymer segments, designated by **P**, were built with a composition of **P** = $C_{214}H_{380}$ (corresponding to nine monomeric units, see Figure S11). For simplicity, the polymer segments have been built without the carbonyl group. Length and bond angles were assigned using the HyperChem Model Build database. Alkyl chains, R1 and R2 (see Figure S11), were arranged in all-trans configuration.
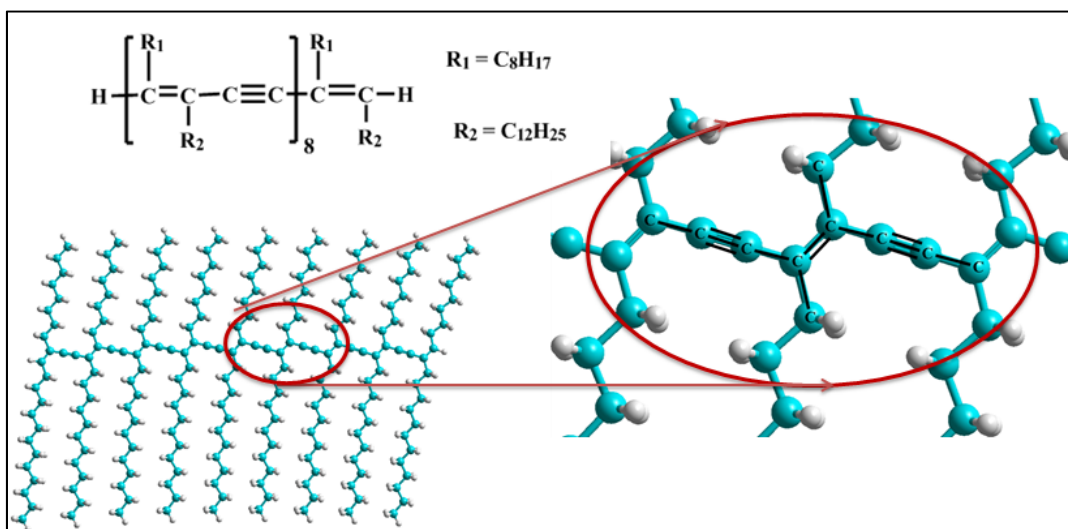


**Figure S11**: Composition of the polymer segment, **P**, used for the study of the PDA system.

The different polymer conformations may be identified by the torsion angles $\theta_\alpha$ and $\theta_\beta$. Thus, $\theta_\alpha$, is the torsion angle formed by the atoms; C=C—$C_\alpha$—$C_\alpha$', (see Figure S12), and $\theta_\beta$, is defined respect to atoms C=C—$C_\beta$—$C_\beta$'. For the initial structures of the polymer segments **P**, the same $\theta_\alpha$ and $\theta_\beta$ values were fixed for every C=C double bonds.
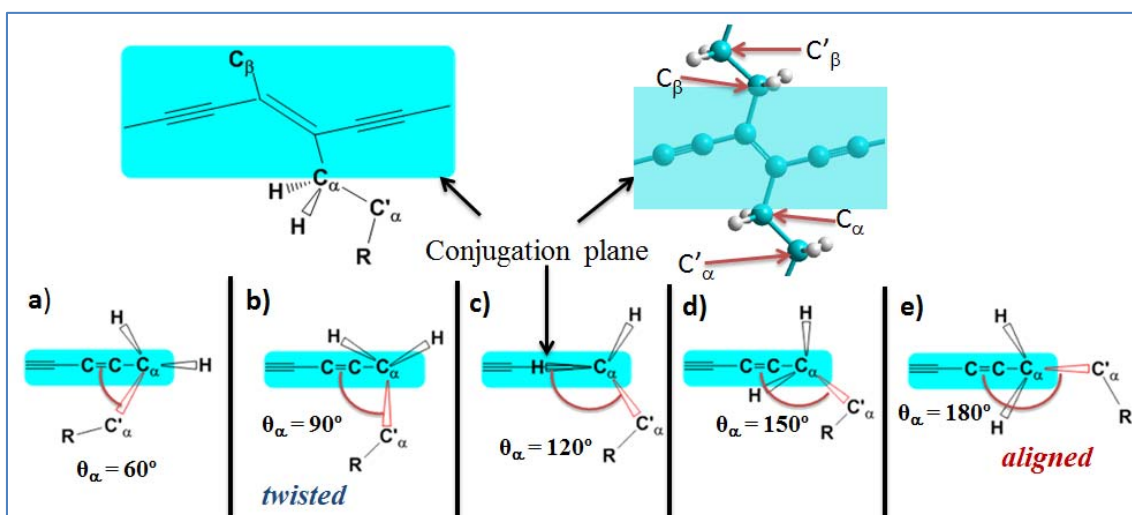


**Figure S12**: Definition of the torsion angles formed by the atoms; C=C—$C_\alpha$—$C_\alpha$', ($\theta_\alpha$), and C=C—$C_\beta$—$C_\beta$' ($\theta_\beta$). Different initial structures of **P** involving the modification of $\theta_\alpha$ = $\theta_\beta$ from 60° to 180° in 30° steps (a-e).

Five different initial structures of **P**, were built, varying $\theta_\alpha = \theta_\beta$ from 60º to 180° in steps of 30° (see Figure S12a-e). Thus, for the *aligned* conformation $\theta_\alpha = \theta_\beta = 180°$ (see Figure 12e), while for the *twisted*, $\theta_\alpha = \theta_\beta = 90°$ (see Figure 12b). Once built, the charge values were introduced via the semi empirical AM1 method (single point) for the **P** polymer segments once they were built into the desired conformation. Figure S10 (lower left) shows one of these segments for the *aligned* configuration.

Clusters of eight **P** polymer segments are positioned parallel and separated ca. 0.4 nm, then proceeding to the geometric optimization using the molecular mechanics MM+ method including no cut-offs. The Polak-Robiere method was used for minimizing the energy. The convergence criteria was 0.001 kcal/(Å·mol). For each initial conformation, all the optimization process was repeated four times; small displacements of the initial position and relative distance of the polymers segments were included.

Starting conformations have angle values of $\theta_\alpha = \theta_\beta = 60º$, $\theta_\alpha = \theta_\beta = 90º$, or $\theta_\alpha = \theta_\beta = 120°$ The geometric optimization led to conformations with $\theta_\alpha = \theta_\beta = 82° \pm 3°$ (*twisted* conformation), indicating that the conformations that depart from placing hydrogens in the conjugation plane (60º or 120º) are not stable. On the other hand, starting from a conformation in which $\theta_\alpha = \theta_\beta = 150º$ or $\theta_\alpha = \theta_\beta = 180°$ led to a final conformation displaying $\theta_\alpha = \theta_\beta = 175° \pm 5°$ (*aligned* conformation). For the next step, each optimized structure was subjected to four runs of the molecular dynamics simulations to search for the possible existence of other structures with lower energy. Each run includes: heating the structure to 300 K, running molecular dynamics simulations for 4 ps, and finally annealing to 0 K. After each molecular dynamics simulation the structure was again optimized by using MM+. In all cases, after this geometry optimization, the structures obtained retained the starting *aligned* or *twisted* conformations, Therefore no structures with lower energy were found.

Significant results of the different calculations are shown in table S1. The *aligned* and *twisted* conformations seem to represent energy minima and therefore the most efficient packing of the alkyl chains.

| | aligned | Twisted |
|---|---|---|
| $\theta_\alpha$ and $\theta_\beta$ average values | 175° ± 5° | 82° ± 3° |
| Alkyl tilt angle (short chain) (*) | 6°± 3° | 28°± 10° |
| Alkyl tilt angle (long chain) (*) | 8°± 3° | 11°± 4° |
| **P** Energy (PDA segment) (kcal/mol) | 32 ± 4 | -2 ± 1 |
| **P₄-P₅** energy interaction (kcal/mol) | -284 | -257 |
| Total energy for the 8 **P** segment (kcal/mol) | -1849 | -1920 |

**Table S1**: Significant computational results of the *aligned* and *twisted* conformations. (*)We define the alkyl chain tilt relative to the alkyl chain fully upright (all-trans) in the *aligned* configuration.

In Figures 13a-c three different perspectives (front, side and top) of one of the starting structures (*twisted* before optimization) are shown. Figures 13d-f show similar views for the structure obtained after the geometry optimization. Figure S14 shows the structure for *aligned* conformation before the geometric optimization (Fig. S14a-c) and after the optimization (Fig. S14d-f).
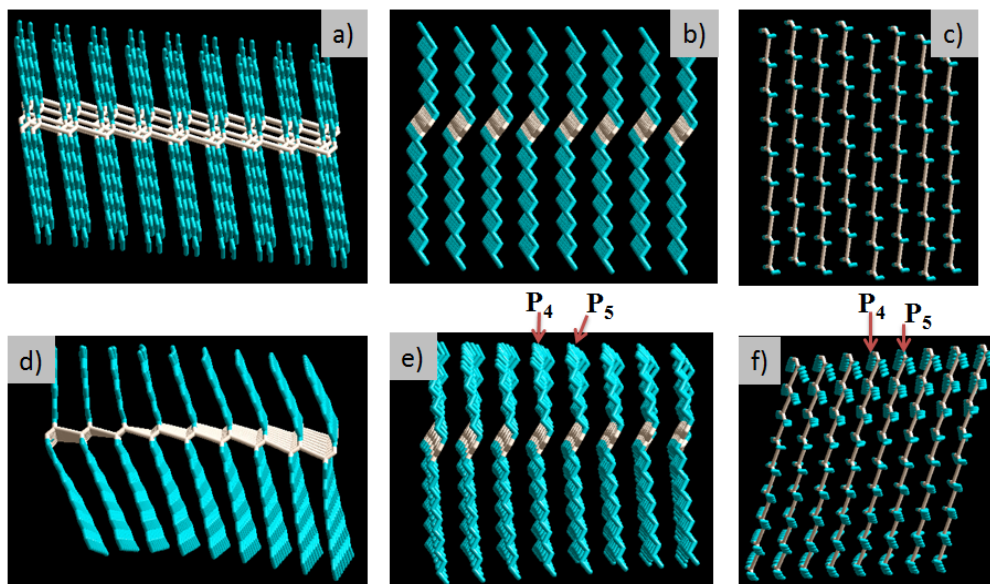
**Figure S13**: Different perspectives (front, side and top) of one of the *twisted* starting structures; a-c) before, and d-e) after the geometrical optimization. The alkyl chains are represented by cyan while the conjugation plane is represented by gray color.



**Figure S14**: Different perspectives (front, side and top) of one of the *aligned* starting structures; a-c) before, and d-e) after the geometrical optimization. The alkyl chains are represented by cyan while the conjugation plane is represented by gray color.
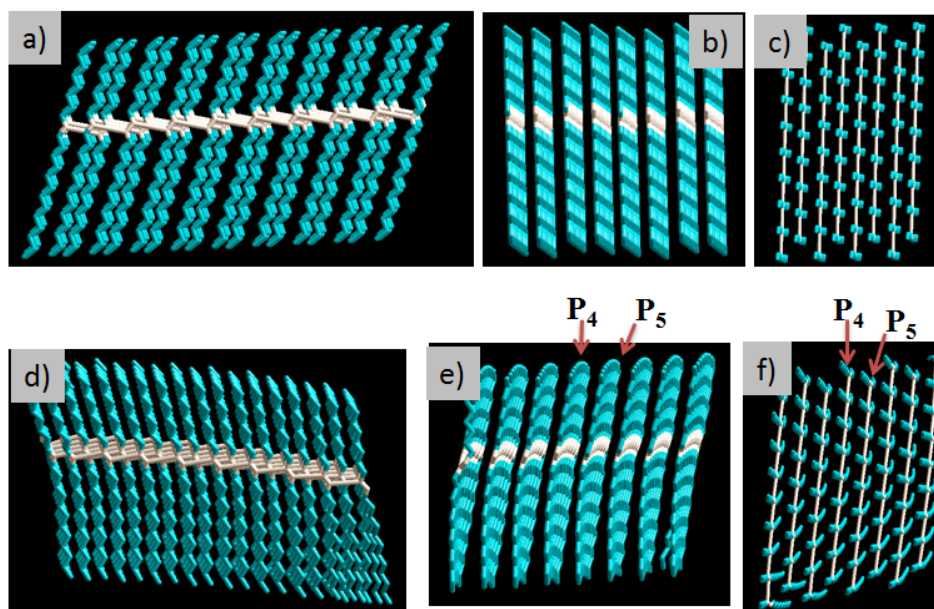
Note the alkyl chains are mainly in all-trans conformation for the optimized conformations, although the chains are partially tilted (see Figures S13d-f and S14d-f). Thus, for the *aligned* conformation the short alkyl chains is tilted 6°, while the long alkyl chain is tilted 8°. Both chains are tilted toward the polymer chain, see Table S1 and Figure S14F. Lifshitz et al. (reference 53 in the manuscript) described the alkyl chains slightly inclined with respect to the air-water interface in the case of the red polymer. Thus, the carboxylate-terminated R1 alkyl chains is tilted 3.5° toward the polymer chain, while the alkyl R2 chain is tilted 5° toward the neighbor polymer backbone direction, implying that both chains are not located exactly on the same plane. On the other hand, for the *twisted* conformation, the short alkyl chain is tilted 11°, while

the long alkyl chain is tilted 28º, with both chains tilted toward the neighbor polymer backbone direction, see Table S1 and Figure S13F. Lifshitz et al. described the alkyl chains with a tilting of 18º and 39º, both toward the neighbor polymer backbone direction, in the case of the blue polymer.

We ascribe the differences between our calculated data and the experimental data from Lifshitz et al. to three possible reasons; (a) The experimental data correspond to the formation of a three-layer, whereas we simulate a single layer. (b) Our model uses the DA monomer units without carboxylic groups, in order to simplify the calculations. The absence of this group as well as the water subphase, can modify the interactions near the polar group, thus leading to a different result. (c) Because the aqueous phase is not simulated, we do not have an air-water interface to define the alkyl chain inclination angle. In this way, we defined the alkyl chain tilt angle relative to the alkyl chain fully upright (all-trans) in the *aligned* configuration.

Small differences in the energies of the different optimized structures for the same final conformation were found. These differences arise from the asymmetric interactions of the external polymer segments. The average energy per **P** polymer segment is provided in Table S1. This energy value is obtained by isolating individual polymer segments after of energy optimization, and then calculating its energy (single point) in the absence of other polymer segments. The energy of the **P** polymer segment in the *twisted* conformation, is ca. 34 kcal/mol more stable than for the *aligned* conformation.

Table S1 additionally provides the interaction energy between two polymer segments (dimer). We selected the central polymer segments of the cluster, designated by **P$_4$** and **P$_5$** in Figure S13 and S14. This energy is obtained by isolating these polymer segments from the optimized structure, determining their energy (single point), and subtracting the obtained energy from the energy of the isolated segments. Note the attraction energy between *aligned* polymer segments is higher than in the *twisted* conformation (ca. 27 kcal/mol).

Our calculations show that the aligned and twisted structures are stable only as a result of interactions with adjacent polymer segments. Polymer segments in the *aligned* conformation are less stable than those of the *twisted* conformation. However, the energy of interaction between segments in the *aligned* conformation is stronger than in the *twisted*. This interaction between the different segments might almost compensate the energy difference, so that these two structures have similar energy minimum. In our reasoning has not been taken into account possible entropic effects. The interactions between polymer segments can be classified as hydrophobic interactions where in the water presence, the entropic factor plays a fundamental role, for example as in the micelle formation. This effect should be similar for both conformations and therefore does not modify the conclusion of our model.

Our results indicate that PDA clusters in *twisted* conformation are slightly more stable than in *aligned* conformation. However, probably increasing the size of the polymer segment considered, or increasing the number of segments in the cluster, the stability ratio could be altered. At this point, the role of the polar group, not considered here, may be critical as well as changes in pH, temperature or interactions with other groups.